Dynamics of electron distributions probed by helium scattering

2009 J. Phys.: Condens. Matter 21 264003

(http://iopscience.iop.org/0953-8984/21/26/264003)

J. Phys.: Condens. Matter **21** (2009) 264003 (9pp) doi:10.1088/0953-8984/21/26/264003

Dynamics of electron distributions probed by helium scattering

M I Trioni[1], G Fratesi[2], S Achilli[2] and G P Brivio[2]

[1] CNISM, UdR Milano-Bicocca, Via Cozzi 53, 20125 Milano, Italy
[2] ETSF, CNISM and Dipartimento di Scienza dei Materiali, Università di Milano-Bicocca, Via Cozzi 53, 20125 Milano, Italy

E-mail: trioni@mater.unimib.it

Received 28 November 2008
Published 11 June 2009
Online at stacks.iop.org/JPhysCM/21/264003

Abstract

Helium atom scattering (HAS) is the most important tool for surface science investigations. The analysis of helium scattering off a solid surface allows for a detailed analysis of its structural and dynamical properties. In this work we show how the dynamics of electron distributions at a metal surface can be investigated by HAS in the adiabatic approximation. First we examine the anticorrugating effect, namely the property of the He–surface potential of those metal systems in which the classical turning points of He beams are farther away from the surface layer at the bridge than at top sites. Anticorrugation for the system He/Cu(111) is examined in detail by a density functional theory (DFT) calculation and compared with the corrugating behaviour of He/Al(111). To explain such an effect the charge polarization of the system is crucial. Second we consider theoretically a surprising restricted diffusion result in the normal direction for Na adatoms on Cu(001) at coverages larger than 0.04 ML, obtained by measurements with spin polarized ^{3}He beams. From DFT calculations for this system a model for the description of the He–surface interaction based on the effective medium theory, which accounts for the observed phenomenon, is discussed. We show that the surface charge distribution probed by HAS is altered by the local concentration of the diffusing adatoms which is fluctuating with time and producing variations in the apparent height of the adatom measured by HAS. Our calculations demonstrate that such electronic dynamical rearrangements can be probed by the ^{3}He spin echo technique, which could be extended to other studies of surface electronic properties.

1. Introduction

Helium atom scattering (HAS) from surfaces has been a fundamental tool for surface science investigations since the experiment of Estermann and Stern who first demonstrated the validity of the de Broglie principle for atoms by diffracting a beam of He using a LiF(001) crystal surface as a diffracting grating [1]. In the 1970s diffraction experiments with He and other atomic and molecular probes were successful on a variety of surfaces [2–5]. There are several advantages to using helium atoms as compared with x-rays, neutrons and electrons and other atoms to probe a surface and study its structures and dynamics. In fact the lightweight He atoms at thermal energies do not penetrate into the bulk of the material being studied. This means that they are strictly surface-sensitive and are truly non-destructive to the sample. Because such atoms have no rotational or vibrational degrees of freedom and no available electronic transitions, only the translational kinetic energy of the incident and scattered beam need be analysed in order to extract information about the surface. Production of the He beam in a high pressure nozzle has allowed velocity spreads of less than 1% to be obtained and the accurate measurement of inelastic events and hence surface phonons [6]. It was also shown that with sufficient energy resolution the quasi-elastic peak of He–surface scattering can probe the lateral diffusion at the surface [7]. In the 1970s pioneering theoretical contributions to the interpretation of elastic and inelastic He–surface scattering were worked out [8, 9], also accounting well for the dispersion of surface phonons [10, 11]. The possible excitations of electron–hole pairs in a He–metal collision in analogy to other non-adiabatic effects at the surface [12, 13] was also considered. But the probability of an inelastic event, due to electron–hole pair excitations, in a rare gas atom scattering at thermal energies off metals was calculated to be negligible [14].

In order to interpret the HAS spectra correctly it is important to describe the static He–surface potential energy $V(\mathbf{R})$, being $\mathbf{R}$ the atomic coordinate, as precisely as possible. The first calculations by first principles within the density functional theory (DFT) in the local density approximation (LDA) were performed by embedding the atom in a uniform electron gas, while the variation of $\mathbf{R}$ was taken into account considering different electron densities, ρ_0. The atom embedding energy, defined as that of the interacting system minus that of the unperturbed electron gas and that of the isolated atom, provides a simple description of the atom–surface energy [15, 16]. This approach represents the so-called effective medium theory (EMT). It is remarkable to note that such embedding energy for noble gas atoms varies linearly with ρ_0, consequently suggesting a proportionality between $V(\mathbf{R})$ and the electron density at the adatom position [17, 18]. This approach provides a reasonable approximation of the repulsive He–metal potential at closer distances from the solid. Owing to its simplicity it was soon necessary to correct it with two terms; one averaging out the non-locality of the interaction, since He is influenced by the charge density over some region, and the other, always negative, accounting for the hybridization between the helium 1s orbital and the excited states of the metal [19, 20]. It is important to observe that the contribution of these two extra terms is different at the top and bridge positions, so that it may happen that the corrugation of $V(\mathbf{R})$ is different from the corrugation of the charge density. For surfaces with weakly varying charge profiles, the corrugation of $V(\mathbf{R})$ may also be opposite from that of the unperturbed charge density of the substrate, hence being larger at the bridge than at top sites (anticorrugating effect) [21]. At atom–surface distances farther away the van der Waals contribution to the He–surface potential becomes important [22]. In order to compute it by DFT it is necessary to go beyond the usual approximations of the exchange–correlation functional. Recently, a unified treatment of the asymptotic van der Waals interaction starting from the so-called adiabatic connection formula and using a local dielectric function was introduced [23]. For He interacting with jellium it calculated the van der Waals coefficient C_3 and the image plane position in good agreement with previous phenomenological results [22].

From the preceding paragraph it is clear that HAS is sensitive to the electronic properties of the atom–surface system and we surmise that it could be employed to have access to such features. This is the main aim of our paper. While our analysis is based on the adiabatic approximation, we show how the repulsive He–surface interaction is mediated by electrons of both the atomic probe and the substrate. In other words helium can no longer be considered an electronically inert probe. HAS is also able to highlight that the electron density does not always follow the ionic substrate positions trivially, and can detect varying surface electronic distributions. We show these features for two phenomena, i.e. anticorrugation and restricted diffusion. In the former atom–surface scattering case the He–metal potential behaves differently from the simple EMT expression, being more repulsive at bridge sites. In the latter phenomenon He scattering is capable of capturing the instantaneous alterations of surface charge densities due to adatom diffusion.

This paper will outline by *ab initio* DFT investigations how the adiabatic dynamics of electrons can be probed by He scattering. In section 2 we shall deal with the anticorrugating effect, while in section 3 we shall explain the apparent motion of Na atoms perpendicular to the surface in Na/Cu(001), observed by ^{3}He spin echo measurements [24, 25]. We will give our conclusions in section 4.

2. The anticorrugating effect

2.1. Generalities

As already pointed out, anticorrugation is a property of the potential describing the interaction of He, or possibly another rare gas atom, with the surface of selected metals, but not of the unperturbed surface charge. The latter is always expected to be corrugated, i.e. with isosurfaces at constant charge in the near surface region displaying maxima at top positions and minima at mid-atomic ones [26]. Instead anticorrugation occurs when, for the same impinging normal kinetic energy, the classical turning point (CTP) of the static He–metal potential, $V(Z)$, as a function of the normal atom–surface coordinate, Z, is closer at the top than at bridge positions of the first surface atomic layer. Anticorrugation, though a weak effect, has stimulated thorough investigations of the bonding of rare gas atoms on solid surfaces. Rare gas adsorption is so sensitive to the approximated exchange–correlation functionals as to make adsorption sites depend on such a choice [27]. In fact more accurate GGA-DFT calculations have confirmed that He, Xe and Kr on Pd(111) adsorb on top sites, in agreement with an anticorrugating trend, while the fcc site is the preferred one for Ne and Ar at variance with LDA results. Recent molecular dynamics simulations have shown that a strong friction drop occurs in anticorrugating systems such as Ar, Kr, Xe on Cu(111) after applying an external load [28].

Anticorrugation was reported first by Rieder, Parschau and Burg on Ni(110)c(2 × 4)H and Rh(110)(1 × 2)H. These authors showed that the corrugation amplitudes measured by helium scattering off the surface display maxima translated by half the interatomic distance with respect to those obtained by Ne. In their experiment (see figure 2 from [21]) the brightest spots refer to H atoms along the [100] direction which fix the reference phase. The measurements clarify that only the Ne maxima follow the true corrugation of the surface [21]. It was also demonstrated by DFT calculations for He and Ne atoms interacting with Al and Ag (jellium-like) surfaces that Ne, due to its larger atomic polarizability, gets closer to the surface than He for the two atomic beams with the same impinging kinetic energy in the experimental range of interest [29, 30]. DFT calculations of $V(Z)$ for a realistic substrate confirmed the experimental result which was accounted for in terms of hybridization between the s and $2p_z$ orbitals of the He atom together with modifications of the d band of the metal near the Fermi level E_F [31]. Such an explanation is probably valid for most metals with a large d density of states (DOS) near E_F. Anticorrugation was phenomenologically invoked to describe satisfactorily the anomalies of the inelastic He scattering

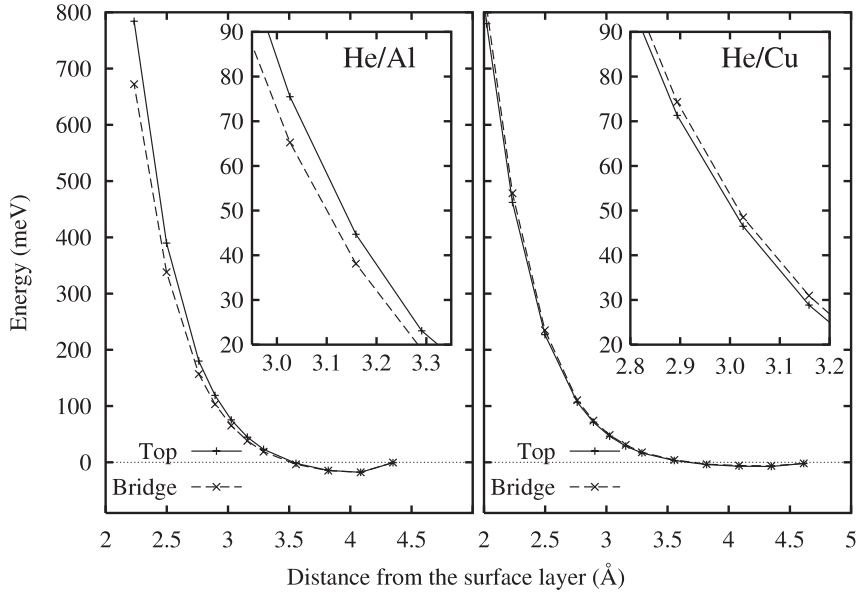

Figure 1. Interaction potential energy for He approaching Al(111) (left) and Cu(111) (right) as function of the distance from the surface layer. The on top and bridge positions are reported with solid and dashed lines, respectively. The inset shows a magnified portion for He energies used in experiments.

spectra for a noble metal surface, i.e. Cu(111), in which all the d band is instead far from E_F [32]. So the explanation proposed in [31] cannot be applied to all these different systems, and a more general analysis of this phenomenon is needed. Here we discuss specifically anticorrugation in Cu(111).

2.2. *Results for He/Cu(111) and He/Al(111)*

Although phenomenological models may still be useful [33], an accurate description of the rare gas–surface interacting system asks for a full DFT calculation for a realistic system. However, it is well known that there are limitations in the standard exchange–correlation functional, which are incapable of accounting for the van der Waals part of the interaction. But they are accurate enough in describing the gas–metal potential at closer distances, where the interaction is repulsive, and in determining the He CTP necessary for scattering simulations. To gain insight it is very interesting to compare results obtained for such potential for a simple surface, Al(111), and a noble metal surface, Cu(111), so often investigated in He–surface experiments.

We carried out the DFT calculation treating exchange–correlation in the PBE generalized gradient approximation [34] and the linearized augmented plane wave (LAPW) basis set using the full potential FLAPW code with a slab geometry [35]. The interaction energy $V(Z)$ is displayed in figure 1 [36]. Note that the calculated attractive part of the potentials is less accurate owing to the poor description of the van der Waals contribution. We can verify that the He–surface repulsive potential is very similar at the top and bridge positions, but the potential on Al(111) is corrugated differently from that on Cu(111) which is instead weakly anticorrugated. In fact, if we assume that a He beam with kinetic energy $E_{kin} = 50$ meV impinges normally onto the above mentioned surfaces, for He/Cu(111) the CTP is slightly closer to the surface at the top position than at the bridge one.

This result is unexpected because the potential does not follow the charge density profile of the clean metal surface, which is corrugated both for Al(111) and Cu(111). In figure 2 we show the contour plots of the electron density of Al(111) in the left panel and of Cu(111) in the right one. Note that the isodensity lines for Cu are closer to the surface than those for Al. Crosses denote the CTP as deduced by figure 1 for $E_{kin} = 50$ meV. At these distances from the surface the corrugation of the charge density is larger for Al (0.05 Å) than that (extremely weak) of Cu (0.02 Å). The values of the corrugation of the potentials are instead 0.04 Å for He/Al(111) and −0.01 Å for He/Cu(111). We point out that both potentials are more repulsive than the EMT one in its simplest formulation [17], defined as

$$V(Z) = \alpha\rho(Z), \tag{1}$$

which predicts that the turning point for $E_{kin} = 50$ meV should be closer to the surface at the charge corresponding to the solid line in figure 2. In the previous equation $\rho(Z)$ is the unperturbed charge density at distance Z from the first metal layer, $\alpha = 300$ eV a_0^3 [37], and the dependence on X and Y is implicitly understood. We also deduce that the terms beyond (1) in the He–surface potential are more repulsive for He/Cu(111) than for He/Al(111), since to reach the CTP He has to penetrate a larger charge density on Al than on Cu.

We now analyse the various contributions to the corrugation of the atom–surface potentials for Al(111) and Cu(111). In table 1 we report the difference of the energies at the top and bridge positions, namely that of the single particle kinetic energy, ΔT_s, that of the classical Coulomb term (electronic plus nuclear), ΔE_{Coul}, and that of exchange–correlation ΔE_{xc}. This analysis is performed for an atom–metal distance of 3.02 Å, which corresponds to the CTP on

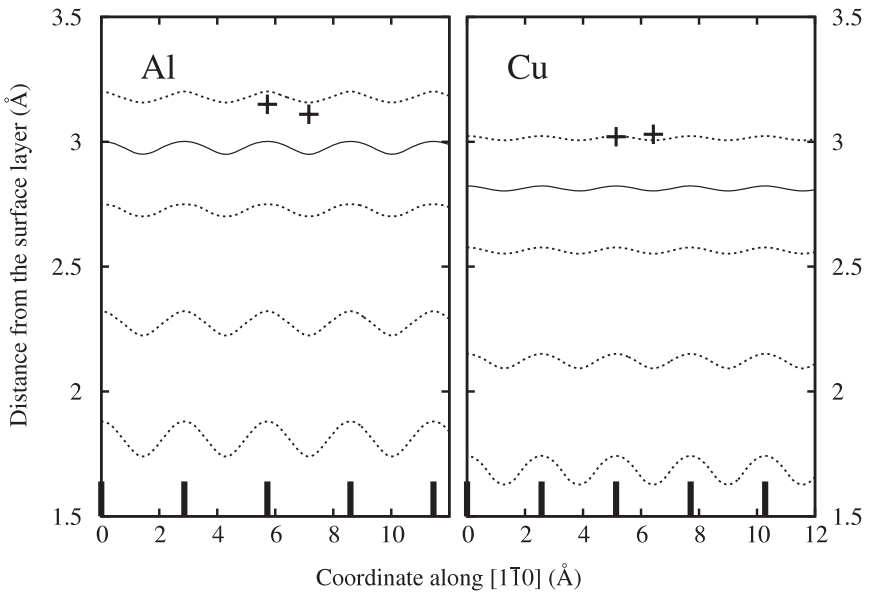

Figure 2. Dotted lines: charge density profile at different values (1.00×10^{-4}, 3.16×10^{-4}, 1.00×10^{-3}, 3.16×10^{-3} a_0^{-3}) for Al(111) (left) and Cu(111) (right) clean surfaces. Solid lines indicate the classical turning point given by EMT for $E_{\rm kin} = 50$ meV (isovalue at 1.67×10^{-4} a_0^{-3}), and crosses the one given by our *ab initio* calculation. Vertical bars mark the position of underlying substrate atoms.

Table 1. Difference of the various energy contributions to the He–metal potential at top and bridge positions. Values in meV.

	He/Cu(111)	He/Al(111)
$\Delta T_{\rm s}$	−26.0	−47.3
$\Delta E_{\rm Coul}$	20.1	67.7
$\Delta E_{\rm Coul+kin}$	−5.8	20.4
$\Delta E_{\rm xc}$	4.1	−10.0
ΔV	−1.7	10.4

the top position on Cu(111) at 50 meV. Observe that $\Delta T_{\rm s}$ is always negative, i.e. it gives an anticorrugating contribution, while $\Delta E_{\rm Coul}$ is positive, contributing instead to the corrugated potential. The fact that $|\Delta T_{\rm s}|$ is larger than $|\Delta E_{\rm Coul}|$ for He/Cu(111), while the opposite occurs for He/Al(111) for which $\Delta E_{\rm Coul}$ dominates, signals the overall property which marks the difference between the anticorrugating behaviour of the former and the corrugating behaviour of the latter system. In other words a relatively larger kinetic energy contribution may help repulsion better at bridge than at top sites for He/Cu(111), while attraction at bridge positions is favoured in He/Al(111) by a stronger positive Coulomb term. We also note that the magnitude of $\Delta E_{\rm xc}$ is the smallest one, having opposite sign with respect the overall behaviour, positive for He/Al(111) and negative for He/Cu(111), and that this term does not influence the qualitative features of corrugation and anticorrugation of the two systems, although it tends to weaken the previous effects.

To examine anticorrugation of the two above mentioned systems in more detail, in figure 3 we report the charge displacement, defined as the total charge of the interacting system minus that of the isolated He and unperturbed metal. The plots on the right of figure 3 show that the interaction induces a dipole fairly localized on the adatom with the electron density displaced towards the surface for He/Cu(111). On the other hand, at the same Z a more complex rearrangement of the electronic charge occurs for He/Al(111) (see left panels of figure 3). In this case there is a stronger intermixing of the electronic charge than in He/Cu(111). This rearrangement is very different from that of previous cases showing a depletion of the electron density which appears more delocalized around the He atom. Furthermore, the differences in the induced charge between top and bridge position are larger on Al(111) than on Cu(111), in which they look very similar.

In order to achieve more insight into such He–metal interactions we perform a calculation of the He/Cu and He/Al charge displacements without including the corrugation of the surface. In this way we wish to discriminate the effects due to the different metals from the effects due to the top and bridge sites. So we take advantage of a simplified surface model, in which He interacts with a non-corrugated metal surface, described by a laterally averaged electron effective potential. This can be realized in a 3D DFT calculation by using a 1D model potential for the substrate as proposed by Chulkov and co-workers [38].

In figure 4 we plot the charge displacement for He/Al (left panel) and for He/Cu (right panel), as a function of the surface normal z and parallel x coordinates. The He–surface distance has been chosen about the CTP as calculated previously for realistic surfaces, i.e. 3.02 Å. On Cu near the He nucleus the closed solid line lobe identifies a positive small electron displacement nearer to the surface and the broken line an electron depletion. So the polarization can be considered as an effect of the effective potential tail of the clean surface whose slope determines an electric field displacing the 1s state of He towards the surface. On Al in contrast the charge rearrangement is more complicate, since the charge redistribution involves not only that of He but also that of the surface. This discrepancy can be ascribed to the different

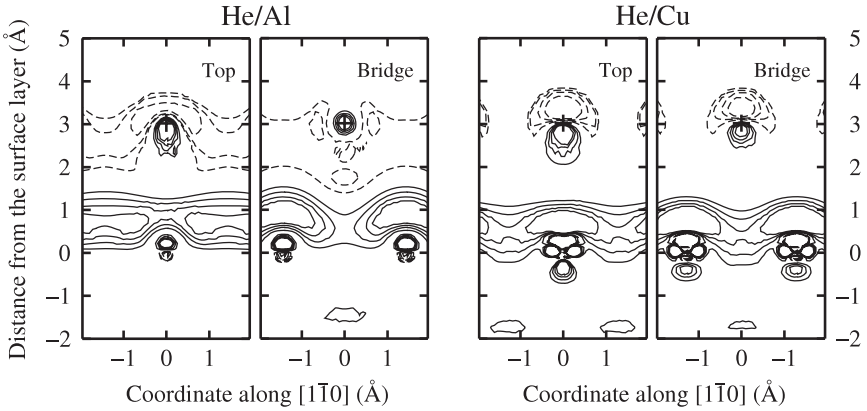

Figure 3. Contour plots of charge displacements for He on Al(111) (left panels) and He on Cu(111) (right panels) for top and bridge positions at atom–surface distance $Z = 3.02$ Å. Full lines denote an increase and dashed lines a decrease in electron density.

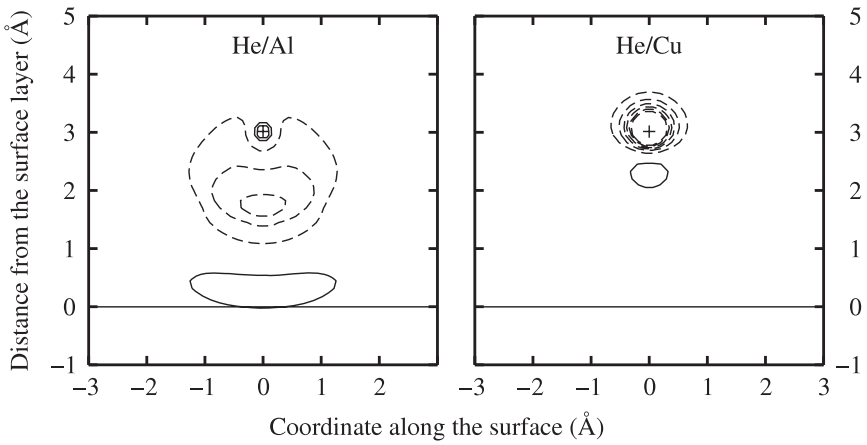

Figure 4. Contour plots of charge displacements for He on Al(111) (left panels) and He on Cu(111) (right panels). The atom–surface distance is $Z = 3.02$ Å and the surface is modelled with a 1D potential (see text). Full lines denote an increase and dashed lines a decrease in electron density.

electronic structure of Al(111) and Cu(111) surfaces. First, the Al band is wider, allowing the 1s level of He to slightly hybridize with metal states, while on Cu the energy of the 1s level of He lies below the bottom of the band. Second, at the surface Brillouin zone centre there are no states at E_F for the Cu(111) surface, differently with respect to Al(111). Both the previous points justify the larger rearrangement of the electron charge on Al(111). Comparison of the charge displacements reported in figure 2 with those in figure 4 shows that for the He/Cu systems both substrate models produce similar charge rearrangements, while for He/Al(111) those obtained at the bridge site are more like those worked out on a flat surface, contrary to the top site results.

In conclusion, for both systems the kinetic energy is anticorrugating and the Coulombic energy is corrugating. While the kinetic energy difference behaves similarly for the two substrates (being larger for Al(111) due to the larger charge density corrugation), the Coulomb energy contribution is larger on Al(111) than on Cu(111), following the larger difference in the charge displacement on Al than on Cu when comparing bridge and top sites. The magnitude of such terms allows one to overcome the anticorrugated kinetic contribution for He/Al(111) but not for He/Cu(111).

3. Restricted diffusion of Na on Cu(001)

3.1. ^{3}*He spin echo results*

In this section we wish to show that HAS is sensitive to instantaneous alterations of the surface charge density and that this occurs in low coverage diffusion experiments. A great improvement in the resolution of the quasi-elastic peak and an increase of about three orders of magnitude of the time evolution with respect to standard HAS for surface processes has recently been obtained by the ^{3}He spin echo technique, a method developed from that of neutron beams [39]. The ^{3}He spin echo apparatus of the Cambridge Surface Science Group can measure phenomena up to 0.4 ns and energy resolutions of the order of 3 μeV [25, 40, 41].

Differently from anticorrugation, in this surface diffusion investigation the hypothesis of an inert He beam is justified and works fairly well (see the following) so that from the scattering spectra we can extract information which solely refers to the surface process and hence determine the potential wells and barriers and the interparticle interaction of the mobile species. Then diffusion is simulated by a classical molecular dynamics calculation with the above input data. But

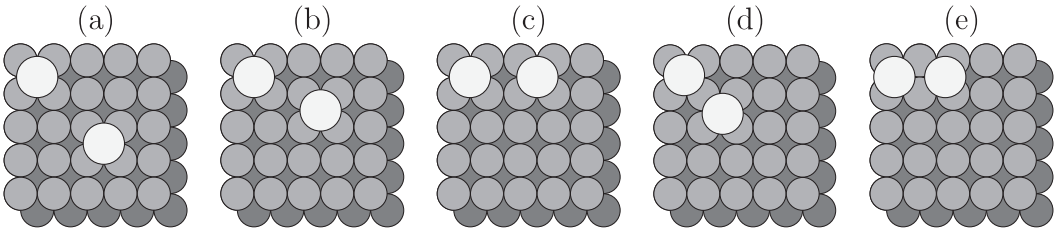

Figure 5. Top view of the possible configurations of two Na adatoms (bright circles) in a Cu(001) (5 × 5) cell.

of course diffusing adsorbed atoms are not rigid balls and complex physical/chemical interactions set in with the metal and among themselves. The scope of this part of the paper is to demonstrate how we can follow the dynamics of the electrons in diffusing adatoms at low coverage by ^{3}He spin echo. Still we assume the adiabatic approximation to be valid, but the local charge density is shown to be at variance with that obtained by summing up the contribution of the adsorbates, being delicately sensitive to the adsorbate configurations.

In particular, our investigation was motivated by the onset of a thermally activated apparent perpendicular motion of Na adatoms on Cu(001), which was inferred from ^{3}He spin echo scattering experiments [25]. For coverages from $\theta \leqslant 0.05$ up to $\theta = 0.08$ they found an anomalous time dependent polarization loss $P(\Delta\mathbf{K}, t)$ for parallel momentum exchange between He and the surface, $\Delta\mathbf{K} \cong 0$, which corresponds to specular reflection. When diffraction occurs with finite $\Delta\mathbf{K}$, $P(\Delta\mathbf{K}, t)$ tends exponentially to zero showing that the width of the pair correlation function $G(\mathbf{r}, t)$, whose Fourier transform is the polarization loss, extends at larger distances for longer time lags between the surface collision of the two spin polarized ^{3}He beams. Since at specular reflection the parallel motion cannot be detected one would expect P not to depend on time. On the contrary, in this coverage range the loss function at $\Delta\mathbf{K} \cong 0$ exhibits a time dependence. In particular, it behaves like that for restricted motion, where the width of the pair correlation function $G(\mathbf{r}, t)$ stops increasing as soon as the particle has explored its available region. Consequently the function $P(\Delta\mathbf{K}, t)$ can be fitted by the form $[\exp(-\alpha t) + C]$, where α is the inverse lifetime of the process and $C > 0$ is a constant. One is led to conclude that an apparent confined perpendicular motion of diffusing Na is present, with a lower bound of 0.2 Å for the extent of the motion. By considering that experiments can detect time lags up to about 0.5 ns, this rules out any adatom–metal vibrational oscillation [42], as well as adatom confinement excludes any Na desorption from the surface. Numerical models in which the height of the Na atom changes depending on the local adsorbate configuration, which in turn fluctuates in time owing to adsorbate diffusion on the surface, reproduced these experimental findings and prompted the search for a connection between the confined perpendicular motion and the unconfined parallel one. An explanation has been found by first-principles techniques, as reported in the following paragraphs.

3.2. DFT calculations and model explanation

Calculations based on DFT, with periodically repeated slabs and adopting the PBE GGA for the exchange and correlation

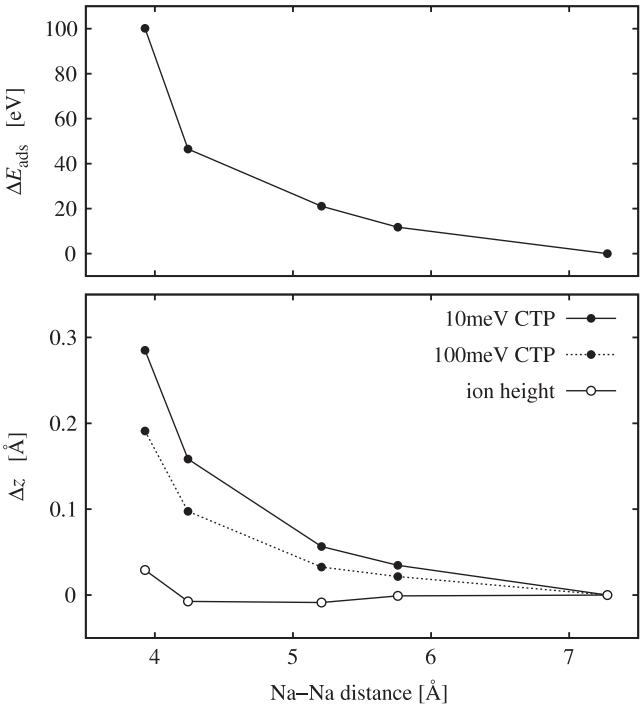

Figure 6. Top panel: adsorption energy per atom for the configurations shown in figure 5. The energy for configuration (a) is chosen as reference. Bottom panel: variation in the Na height with respect to configuration (a). The Na ion height of the latter is 2.35 Å; the classical turning point estimates for kinetic energies of 10 and 100 meV are 5.22 Å and 4.17 Å, respectively, all measured from the position of the first Cu layer of the unperturbed substrate.

functionals, can provide an answer to this unexpected result by estimating the contributions to the perpendicular motion given by alterations in the adsorption coordinate and in the electron distribution [43]. First, we remember that for low Na coverage on Cu(001) Na atoms adsorb in hollow sites, in agreement with the experimental findings [44], and they display a strong dipole moment (up to about 3 D) [45, 46].

To estimate the alterations of the nuclear height depending on the presence of other adsorbates nearby we turn now to two Na atoms per unit cell at $\theta = 0.08$ in a Cu(001) (5 × 5) cell, where five adatom configurations are possible. Such configurations are shown in the five panels in figure 5, and their adsorption energies are plotted in the upper panel of figure 6, choosing the energy for configuration (a) as reference. It is interesting to look at the height of the Na ion (empty balls) in the lower panel of figure 6. Again the reference coordinate is that of the Na ions plotted in panel (a), which amounts to

2.35 Å from the first Cu(001) layer. We can conclude that the various differences in the normal coordinate of the adatoms, ΔZ, by changing their positions in the unit cell, are too small to explain the experimental apparent vertical motion, and we can rule out an effect related to normal displacements of the ionic coordinate.

So we investigate the charge density by changing the relative sites of the two Na adatoms in the unit cell, again for the configurations shown in figure 5. In figure 7, the contours of the valence charge density are reported on a (100) plane passing through the Na atoms, on the right for the (d) configuration and on the left for the (a) one. Already a first glance shows that, when the two adatoms get closer, charge contours of the same magnitude are displaced outwards, suggesting that He atoms will be scattered at larger distances. To make quantitative progress we need a model for the He–metal potential. For this study we can safely use the EMT in its simpler form and define the scattering (repulsive) He–metal potential as in (1), hence not considering the difference between the corrugation of the He–surface potential and that of the surface charge density, which were the focus of section 2. Indeed, in this case we are interested in differences in the turning point at the same site (atop the Na adatom), so that the He atom can be assumed to behave similarly independently of the local concentration; furthermore, the apparent vertical Na displacement is about ten times that of the corrugation difference between top and bridge positions, calculated for He scattering off Cu(111) at the same incoming He kinetic. We then describe the scattering process classically and define the classical turning point, Z^{CTP}, for fixed E_{kin} by imposing the condition

$$V(Z^{\mathrm{CTP}}) = E_{\mathrm{kin}} \cos^2(45^\circ/2), \tag{2}$$

where $E_{\mathrm{kin}} = 10$ meV is the experimental kinetic energy of the impinging He and 45° is the scattering angle [25]. Such an approximation may be questionable owing to the small He kinetic energy, but, as we shall see, the results are robust by varying E_{kin}. Let us look at the magnification of the inset in figure 7, i.e. the bottom panel in the same figure, which displays the charge contours on top of a Na adatom and highlights the position of the CTP. For a He kinetic energy equal to the experimental value, the charge contours of the same magnitude are farther away from the surface if the adatoms are closer (configuration (d) of figure 5) than those of configurations (a) (adatoms more distant on the surface). This effect is fairly robust as shown by increasing E_{kin}: it decreases by about 50% for $E_{\mathrm{kin}} = 100$ meV but is still much more significant than the variation in the nuclear coordinate. A detailed analysis proves that for $E_{\mathrm{kin}} = 10$ meV the turning point of He increases smoothly from 5.2 Å above the Cu–surface atoms from the configuration in figure 5(a) up to 5.5 Å for the configuration in figure 5(e), a variation of the same magnitude as the observed perpendicular motion. This is shown in the bottom panel of figure 6 and is to be compared to the negligible alterations in the adsorption coordinate previously discussed. Consequently the apparent height measured by He is related to the local charge protruding from the surface and hence to the local configurations of the diffusing Na, though at (average) constant coverage on Cu(001), and this is only due to electronic contributions.

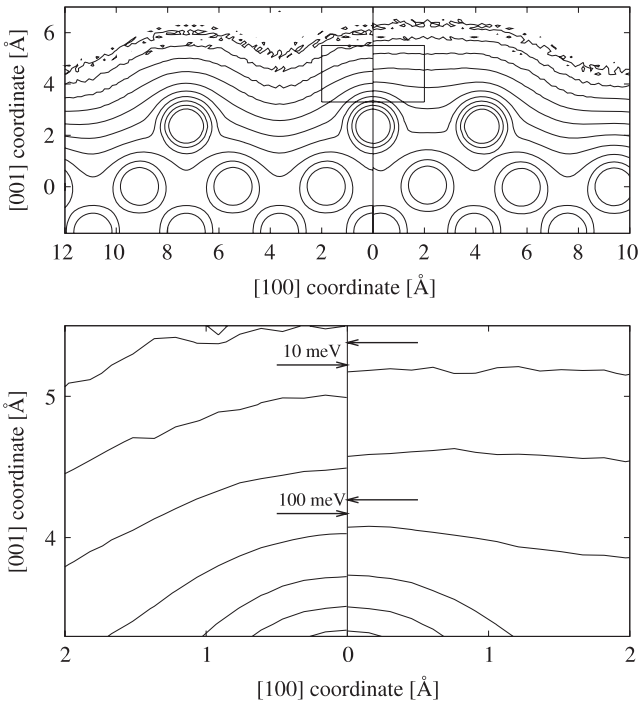

Figure 7. Valence charge density on a (100) plane passing through the Na atoms. Data for the structures (a) and (d) are shown on the left- and right-hand side of each panel, respectively. The bottom panel is an enlargement of the rectangle in the top one. Here, the arrows mark the position of our estimate for the Na height for kinetic energies of 10 and 100 meV (charge density of 1.92×10^{-4} and 1.92×10^{-3} Å^{-3}). Contours are drawn in logarithmic scale at the following densities: 3.16×10^{-5}, 1.00×10^{-4}, 3.16×10^{-4}, . . ., 1.00 Å^{-3}.

We have verified that this is a systematic effect present in more general cases than the ones depicted in figure 5 by taking into account the computationally more demanding task to introduce more adatoms in larger supercells: we have simulated (5 × 10) supercells with four Na atoms (0.08 ML) and two Na atoms (0.04 ML). In such cases the number of Na arrangements is much larger. Then, as before, we have computed the electron density by DFT and worked out the EMT estimate of the Na apparent height. The results confirm the previous range of CTPs for the same impinging He kinetic energy and can be analysed quantitatively by using a suitable measure for the local concentration. For convenience, we choose the same measure as in [25], namely the dipole–dipole interaction energy per atom, E_i^{dd} [47]:

$$E_i^{\mathrm{dd}} = \frac{1}{2}{\sum_j}' \frac{2\mu_{\mathrm{ave}}^2}{|\mathbf{R}_i - \mathbf{R}_j|^3}. \tag{3}$$

Here i and j label adatoms with nuclei in $\mathbf{R}_i$ and $\mathbf{R}_j$, the summation ranges over all Na atoms j different from i. Within the supercell approach, periodic replicas are also to be included; μ_{ave} is the average dipole of Na adatoms, the factor 2 accounts for interaction with image charges. Hartree atomic units are used here and onwards unless differently

specified. By considering several local concentrations which can be explored by the large (5 × 10) supercells, we are able to prove a relationship between Z^{CTP} and E_i^{dd} which increases linearly and with larger slope for $\theta = 0.08$ (3.36 Å eV^{-1}) than for $\theta = 0.04$ (2.66 Å eV^{-1}).

This linear dependence can in turn be used in MD simulations to obtain the probability distribution of the apparent height of Na starting from that of the dipole–dipole interaction energy per atom, which is routinely evaluated. At temperatures $T = 155$ K as in the experiment we have obtained a fairly broad probability distribution of apparent Na height, showing a full width at half maximum (FWHM) equal to 0.14 Å at $\theta = 0.08$, and a narrower distribution (FWHM = 0.07 Å) for $\theta = 0.04$, in agreement with the experimental results.

Finally, we show by a simple model that the dependence of the CTP on the local Na concentration arises mainly from changes in the potential acting on the electrons, V_{KS}. To do so, we label first $\mathbf{R}_0 = (X_0, Y_0, Z_0)$ the coordinate of a Na nucleus and consider points above it normal to the surface, for values $z \approx Z^{\mathrm{CTP}}$. At low Na coverage, the dominant contribution to V_{KS} by other Na atoms is the dipole electrostatic potential, V_{d}, which for small $z - Z_0$ is given by

$$V_{\mathrm{d}}(z) \approx \sum_j{}' \frac{2\mu_{\mathrm{ave}}(z - Z_0)}{|\mathbf{R}_0 - \mathbf{R}_j|^3} = \frac{2(z - Z_0)}{\mu_{\mathrm{ave}}} E_0^{\mathrm{dd}}. \tag{4}$$

Since the electron charge $\rho(z)$ into the vacuum is well described by an exponential function, within the Wentzel–Kramers–Brillouin approximation, we can write

$$\rho(X_0, Y_0, z) \approx \rho_0 \exp\left(-2k(z - Z_0)\right), \tag{5}$$

where

$$k = \sqrt{2(V_{\mathrm{KS}} - \epsilon)}, \tag{6}$$

and ϵ is the average energy of the states contributing to ρ. The CTP is determined by inverting (5) for the charge density, ρ_{EMT}, corresponding to (1) and (2):

$$Z^{\mathrm{CTP}} = Z_0 + \frac{1}{2k} \log\left(\frac{\rho_0}{\rho_{\mathrm{EMT}}}\right). \tag{7}$$

By composite differentiation and use of (4), (6) and (7), one obtains the rate

$$R_{\mathrm{Na}} \equiv \frac{\partial Z^{\mathrm{CTP}}}{\partial E_0^{\mathrm{dd}}} = \frac{\partial Z^{\mathrm{CTP}}}{\partial k} \frac{\partial k}{\partial V_{\mathrm{KS}}} \frac{\partial V_{\mathrm{KS}}}{\partial E_0^{\mathrm{dd}}} = \frac{2(Z^{\mathrm{CTP}} - Z_0)^2}{\mu_{\mathrm{ave}} k^2}, \tag{8}$$

where Z^{CTP}, k and μ_{ave} are easily estimated by a single DFT calculation at the given coverage. For $\theta = 0.08$ ML, $R_{\mathrm{Na}} = 2.67$ Å eV^{-1}, in good agreement with the result by fitting the DFT data, i.e. 3.36 Å eV^{-1}. Moreover the simple formula in (8) determines, as expected, a reduction of the rate by increasing the He kinetic energy or decreasing the coverage.

4. Conclusions

In this paper we have outlined how helium scattering is sensitive to the surface electronic structure. First of all we have discussed the anticorrugating effect; though such an effect is a weak one it can be shown that for transition metals with a large 3d density of states at the Fermi level or for noble ones such as Cu(111) with a low charge corrugation, the interaction between He and the metal is not that between an inert gas atom and the surface, but that an electronic charge rearrangement influences the overall charge distribution of the system. In this way the He–surface interaction changes its effective phase of π, displaying classical turning points farther away from the surface at bridge than at top sites, for the same normal He kinetic energy. We presented an interpretation of this effect based on a DFT calculation, which also provides detailed graphs of the charge polarizations for a corrugated, He/Al(111), and anticorrugated, He/Cu(111), system. The different features of the charge displacements of the two systems can qualitatively account for the corrugating and anticorrugating behaviour of He/Al(111) and He/Cu(111) potentials, respectively.

More recently, the ^{3}He spin echo apparatus has been shown to be capable of measuring surface phenomena with time lags up to 0.4 ns. Low coverage diffusion measurements of Na/Cu(001) have outlined an unexpected effect, namely an apparent vertical and restricted motion of Na adatoms measurable when the parallel momentum exchange of ^{3}He tends to zero. The theoretical and computational analyses have provided an explanation, based on a purely electronic effect due to fluctuations in the local concentration of Na atoms at fixed coverage following adatom diffusion on the surface. This indeed affects the local charge density of the system and consequently results in a distribution of apparent vertical heights. Differently from anticorrugation, the EMT and a classical analysis of scattering for the repulsive He–surface potential suffice for the description of He probe–surface interaction, since the variations of the CTP above Na atoms are much larger than possible anticorrugating contributions. As already pointed out, the results obtained by ^{3}He spin echo reflect purely electronic properties of the surface. In practice, the probe is able to follow adiabatically all electron modifications which occur instantaneously owing to adatom surface diffusion. In the same way the DFT calculations account for differences in local Na concentration in large enough cells, and the classical molecular simulations, starting from the *ab initio* electronic parameters, for the experimental apparent vertical height. Finally we remark that a strong adatom dipole is central to this effect so that we may expect to find a similar behaviour for other alkali adatoms as well.

Acknowledgments

This work was supported by the EU Network of Excellence NANOQUANTA (grant no. NMP4-CT-2004-500198) and the MIUR of Italy (grant No.2005021433-003).

References

[1] Estermann I and Stern O 1930 *Z. Phys.* B **61** 95
[2] Weinberg W H and Merrill R P 1970 *Phys. Rev. Lett.* **25** 1198

[3] Schutte A, Bassi D, Tommasini F and Scoles G 1975 *J. Chem. Phys.* **62** 600
[4] Boato G, Cantini P and Tatarek R 1976 *J. Phys. F: Met. Phys.* **6** 2237
[5] Cardillo J M and Becker G E 1978 *Phys. Rev. Lett.* **40** 1148
[6] Brusdeylins G, Doak R B and Toennies J P 1983 *Phys. Rev.* B **27** 3662
[7] Frenken J W M, Toennies J P and Wöll Ch 1988 *Phys. Rev. Lett.* **60** 1727
[8] Cabrera N, Celli V, Goodman F O and Manson R 1970 *Surf. Sci.* **19** 67
[9] Garibaldi U, Levi A C, Spadacini R and Tommei G E 1976 *Surf. Sci.* **55** 40
[10] Benedek G 1975 *Phys. Rev. Lett.* **35** 39
[11] Bortolani V, Nizzoli F and Santoro G 1978 *Phys. Rev. Lett.* **41** 39
[12] Brivio G P and Grimley T B 1977 *J. Phys. C: Solid State Phys.* **10** 2351
[13] Brivio G P and Grimley T B 1979 *Surf. Sci.* **89** 226
[14] Gunnarssonn O and Shönhammmer K 1982 *Phys. Rev.* B **25** 2514
[15] Nørskov J K and Lang N D 1980 *Phys. Rev.* B **21** 2131
[16] Stott M J and Zaremba E 1980 *Phys. Rev.* B **22** 1564
[17] Esbjerg N and Nørskov J K 1980 *Phys. Rev. Lett.* **45** 807
[18] Puska M J, Nieminen R M and Manninen M 1981 *Phys. Rev.* B **24** 3037
[19] Annett J F and Haydock R 1984 *Phys. Rev.* B **29** 3773
[20] Annett J F and Haydock R 1984 *Phys. Rev. Lett.* **53** 838
[21] Rieder K H, Parschau G and Burg B 1993 *Phys. Rev. Lett.* **71** 1059
[22] Zaremba E and Kohn W 1976 *Phys. Rev.* B **13** 2270
[23] Hult E, Ryberg H, Lundqvist B I and Langreth D C 1999 *Phys. Rev.* B **59** 4708
[24] Jardine A P, Dworski S, Fouquet P, Alexandrowicz G, Riley D J, Lee G Y H, Ellis J and Allison W 2004 *Science* **304** 1790
[25] Alexandrowicz G, Jardine A P, Hedgeland H, Allison W and Ellis J 2006 *Phys. Rev. Lett.* **97** 156103
[26] Brivio G P and Trioni M I 1999 *Rev. Mod. Phys.* **71** 231
[27] Da Silva J L F and Stampfl C 2008 *Phys. Rev.* B **77** 045401
[28] Righi M C and Ferrario M 2007 *Phys. Rev. Lett.* **99** 176101
[29] Montalenti F, Trioni M I, Brivio G P and Crampin S 1996 *Surf. Sci.* **364** L595
[30] Trioni M I, Marcotulio S, Santoro G, Bortolani V, Palumbo G and Brivio G P 1998 *Phys. Rev.* B **58** 11043
[31] Petersen M, Wilke S, Ruggerone P, Kohler B and Scheffler M 1996 *Phys. Rev. Lett.* **76** 995
[32] Santoro G, Franchini A, Bortolani V, Mills D L and Wallis R F 2000 *Surf. Sci.* **478** 99
[33] Nyeland C and Toennies J P 2006 *Chem. Phys.* **321** 285
[34] Perdew P, Burke K and Ernzerhof M 1996 *Phys. Rev. Lett.* **77** 3865
[35] http://www.flapw.de
[36] Jean N, Trioni M I, Brivio G P and Bortolani V 2004 *Phys. Rev. Lett.* **92** 013201
[37] Manninen M, Nørskov J K, Puska M J and Umrigar C 1984 *Phys. Rev.* B **29** 2314
[38] Chulkov E V, Silkin V M and Echenique P M 1999 *Surf. Sci.* **437** 330
[39] Dekiviet M, Dubbers D, Shmidt C, Sholtz D and Spinola U 1995 *Phys. Rev. Lett.* **75** 1919
[40] Fouquet P, Jardine A P, Dworski S, Alexandrowicz G, Allison W and Ellis J 2005 *Rev. Sci. Instrum.* **76** 053109
[41] Alexandrowicz G and Jardine A P 2007 *J. Phys.: Condens. Matter* **19** 305001
[42] Senet P, Toennies J P and Witte G 1999 *Chem. Phys. Lett.* **299** 389
[43] Fratesi G, Alexandrowicz G, Trioni M I, Brivio G P and Allison W 2008 *Phys. Rev.* B **77** 235444
[44] Brivio G P, Butti G, Caravati S, Fratesi G and Trioni M I 2007 *J. Phys.: Condens. Matter* **19** 305005
[45] Graham A P, Hofmann F, Toennies J P, Chen L Y and Ying S C 1997 *Phys. Rev. Lett.* **78** 3900
[46] Ellis J, Graham A P, Hofmann F and Toennies J P 2001 *Phys. Rev.* B **63** 195408
[47] Cucchetti A and Ying S C 1999 *Phys. Rev.* B **60** 11110